Packing Analysis of Organic Crystals Containing C=O or C≡N Groups

A. Gavezzotti

Dipartimento di Chimica Fisica ed Elettrochimica e Centro CNR, Universitâ di Milano, 20133 Milano, Italy
(Received: September 20, 1989)

Eighty crystal structures for organic molecules containing one C=O group, and 13 crystal structures for molecules containing one C≡N group, with up to 20 non-hydrogen atoms, have been retrieved from the Cambridge Structural Database. The effects of the introduction of the polar substituent on the hydrocarbon substrate have been studied by computing packing energies, their correlation to molecular size, and their apportioning into contributions from each atom in the molecule. The reciprocal orientation of the C=O or C≡N dipoles in the crystal has also been analyzed; they never point at each other with the negative charge first. Electrostatic packing energy calculations, in the dipole–dipole approximation, reveal that quite often this energy is negligible and that dipole–dipole interactions are feeble. Centrosymmetric space groups are less frequent in these crystals than in hydrocarbon crystals, and the conditions for formation of head-to-tail pairs between molecular dipoles are discussed. It appears that other cohesive forces can easily overcome this tendency.

Introduction

In recent work,[1,2] the crystal packing of hydrocarbon molecules was examined by a statistical analysis of its geometrical and energetic factors. Relationships between crystal density, packing efficiency, and packing energy were studied as a function of molecular size and shape. Some physical properties of crystals were estimated by empirical formulas. Studies on the forces governing crystal packing are relevant for the prediction of crystal structure (and hence crystal properties) from molecular structure, but also to other fields of chemical research, like protein folding, drug design, or site–receptor interactions, since the same forces are at stake whenever the mutual recognition of molecular objects is involved.

An obvious extension of the previous work on hydrocarbons is the introduction of polar centers and the study of the influence of molecular polarity on packing. The question of the attribution of point charges to atoms in molecules, or of distributed multipoles to simulate the electrostatic potential, has been discussed in a vast literature, together with the methods for the calculation of the pertinent contributions to the packing energy.[3] We deal in this paper with monoketones and mononitriles, that is, molecules bearing an easily identifiable polarization of the molecular electrostatic potential, which is negative around an oxygen or nitrogen atom. This paper describes the results of a statistical analysis of the packing geometries, and, to a less accurate extent, of packing forces in crystals of such molecules.

Data Retrieval and Calculations

The Cambridge Structural Database was searched[4] for crystal structures of molecules containing one C=O or C≡N group; in order that the effects of the polar center be noticeable, the total number of non-hydrogen atoms in the molecule was not allowed to exceed 20. For carbonyl compounds, the initial search yielded 117 hits; after discarding a few disordered structures, as well as structures with more than one molecule in the asymmetric unit (see below), a database of 80 molecules with complete crystal structure information was established. Twenty-one molecules mainly contained aromatic substituents, 25 contained essentially aliphatic groups, 17 contained a mixture of aromatic and aliphatic moieties, and 17 were strained-ring or cage compounds. Using the same criteria, 13 molecules with one C≡N group were retrieved. Table I (supplementary material; see paragraph at the end of this article) contains the CSD refcodes.

The same molecular and crystal descriptors defined for hydrocarbons[1,2] were then calculated (see also the Appendix): molecular van der Waals volume, surface and effective surface;[2] crystal density and packing coefficient; and the packing potential energy, PPE. This last quantity was computed by using nonbonded atom–atom interaction potentials, taken from a repertory[5] whose use and merits have been previously discussed.[6] The reasons for not using more up to date (and presumably more efficient) potential parameters[7] have also been thoroughly discussed.[1] In addition, a dipole–dipole crystal energy, E_{DD}, was calculated[8] (see the Appendix). E_{DD} has obviously no absolute meaning, because the potential functions here employed to calculate the lattice energy are in principle self-sufficient and do not require the presence of specific terms for Coulomb-type interactions. E_{DD} is here used essentially for its relationship with the geometrical features (distance and mutual orientation) of dipoles in crystals. For technical reasons, connected with the operation of computer programs, this contribution could not be computed for crystals with more than one dipole in the asymmetric unit.

The mutual orientation of the dipoles defined by the C=O or C≡N bond vectors was described (see Figure 1) by the following quantities: R_D, the distance between dipole midpoints in the crystal; θ, the angle between the dipole directions in the crystal; and α_1 and α_2, called offset angles. If $\theta = 0$ or 180°, then $\alpha_1 = \alpha_2$ or $\alpha_1 = 180° - \alpha_2$, respectively, and the dipole directions are coplanar. The above four parameters fully describe the geometry of the dipole–dipole interaction, since the dipole length is very nearly constant (averages 1.217 Å for C=O, 1.139 Å for C≡N, quite close to the respective literature average values[9]). All the calculations were performed using previously described[10] techniques, and the statistical treatment was carried out using previously tested[1,2] methods.

Statistics on Overall Packing Indices

Table II reports some average values of physical properties of carbonyl and nitrile crystals, as compared with corresponding averages for crystals of hydrocarbon molecules with up to 20 carbon atoms (a subset of the sample of ref 1). There are no significant differences in the average densities, while the three indices of efficient packing (C_K, the Kitaigorodski packing coefficient; K_0, the bulk modulus at zero pressure; and λ_T, the

(1) Gavezzotti, A. *J. Am. Chem. Soc.* **1989**, *111*, 1835.
(2) Gavezzotti, A. *Acta Crystallogr., Sect. B*, in press.
(3) See for example: (a) Price, S. L.; Stone, A. J. *J. Chem. Phys.* **1987**, *86*, 2859. (b) Williams, D. E.; Starr, T. L. *Comput. Chem.* **1977**, *1*, 173. (c) Gavezzotti, A. *Chem. Phys. Lett.* **1989**, *161*, 67.
(4) Allen, F. H.; Bellard, S.; Brice, M. D.; Cartwright, B. A.; Doubleday, A.; Higgs, H.; Hummelink, T.; Hummelink-Peters, B. G.; Kennard, O.; Motherwell, W. D.; Rodgers, J. R.; Watson, D. G. *Acta Crystallogr., Sect. B* **1979**, *35*, 2331.
(5) Mirsky, K. V. In *Computing in Crystallography. Proceedings of an International School on Crystallographic Computing*; Delft University Press: Twente, The Netherlands, 1978; pp 169–182. See also the Appendix.
(6) Gavezzotti, A.; Simonetta, M. *Chem. Rev.* **1982**, *82*, 1.
(7) (a) Cox, S. R.; Hsu, L.-Y.; Williams, D. E. *Acta Crystallogr., Sect. A* **1981**, *37*, 293, for O···O interactions. (b) Williams, D. E.; Cox, S. R. *Acta Crystallogr., Sect. B* **1984**, *40*, 404, for N···N interactions.
(8) Gavezzotti, A.; Simonetta, M. *Acta Crystallogr., Sect. A* **1976**, *32*, 997.
(9) Allen, F. H.; Kennard, O.; Watson, D. G.; Brammer, L.; Orpen, A. G.; Taylor, R. *J. Chem. Soc., Perkin Trans. 2* **1987**, S1.
(10) (a) Gavezzotti, A. *J. Am. Chem. Soc.* **1983**, *105*, 5220. (b) Gavezzotti, A. *J. Am. Chem. Soc.* **1985**, *107*, 962.

0022-3654/90/2094-4319$02.50/0

TABLE II: Averages (σ) of Density, Packing Coefficient, Bulk Modulus, and Reduced Thermal Conductivity for Groups of Crystals

group	no. of entries	D_c, g/cm^3	C_K	K_0[a]	λT[a]
hydrocarbons[b]	391	1.198 (102)	0.717 (28)	6.17 (127)	1.32 (21)
hydrocarbons $N_C \leq 20$	175	1.162 (95)	0.714 (29)	6.59 (108)	1.36 (17)
C=O crystals	80	1.173 (84)	0.704 (23)	6.10 (109)	1.27 (16)
C≡N crystals	13	1.157 (91)	0.698 (23)	5.83 (86)	1.20 (15)

[a] See Appendix for definition and units. [b] From ref 1.

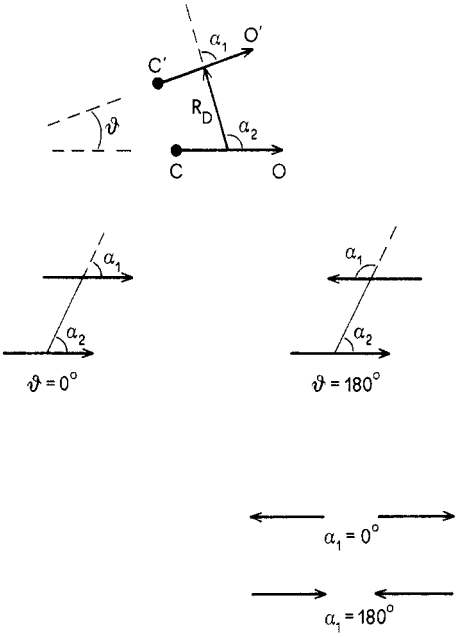

Figure 1. Definition of the geometrical parameters describing the mutual orientation of dipoles. Primed atoms belong to a dipole generated by crystal symmetry from the reference (unprimed) one. For $\theta = 0°$, $\alpha_1 = \alpha_2$; for $\theta = 180°$, $\alpha_1 + \alpha_2 = 180°$.

reduced thermal conductivity) all show a slight decrease on going from hydrocarbons to polar substances. Table III reports the least-squares parameters for the straight lines for PPE against various indices of molecular size; the slopes for S_M, Z_V, and V_M are smaller for polar compounds than for hydrocarbons (another indication of less efficient packing). Differences are, however, barely significant. The slope of the straight line for PPE against the effective molecular surface is quite the same for polar and for hydrocarbon compounds: the corresponding plot is shown in Figure 2. It is the best correlation found for PPE with a molecular size indicator; outliers, both in excess and in defect, follow the trends found for hydrocarbon molecules.[1]

TABLE III: Parameters a_1 and a_2 (σ's) for PPE = $a_1X + a_2$ (kcal/mol; 7-Å Cutoff)

X[a]	a_1	a_2	S[b]
S_M	0.120 (6)	11.2 (15)	3.75
	0.104 (11)	13.3 (28)	3.78
Z_V	0.343 (14)	12.6 (12)	3.32
	0.286 (28)	14.8 (24)	3.57
V_M	0.125 (6)	13.6 (12)	3.53
	0.106 (11)	16.2 (25)	3.76
S_{eff}	0.116 (6)	6.4 (18)	3.88
	0.116 (9)	4.0 (28)	3.14

[a] For each X, upper row is for hydrocarbon crystals with $N_C < 20$, lower row for crystals of carbonyl compounds. [b] Rms deviation.

Figure 3 shows a graph for PPE against the number of carbon atoms in the molecule. As for hydrocarbons,[2] molecules with an even number of non-hydrogen atoms have higher PPE's. If this is to be ascribed to an increase in molecular symmetry, then, the nitrogen or oxygen atom being unique, one must conclude that these atoms must lie on molecular symmetry elements. In order to achieve a higher PE, a molecule must be symmetrical around the C=O or C≡N group.

Energy Partitioning and Intermolecular Contacts. Table IV shows the partitioning of the total PPE in contributions from each atom in the molecule, E_i. There are no significant differences either in absolute values or in trends with the hydrocarbon values.

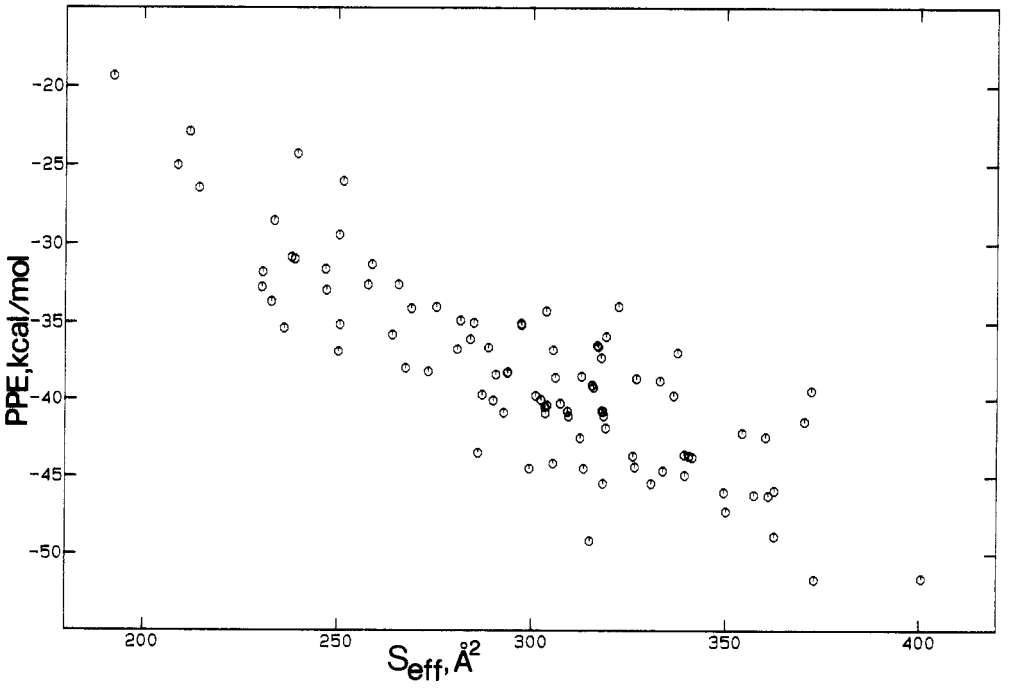

Figure 2. Plot of PPE versus the effective molecular surface (calculated as described in the Appendix) for 93 compounds with C=O or C≡N groups.

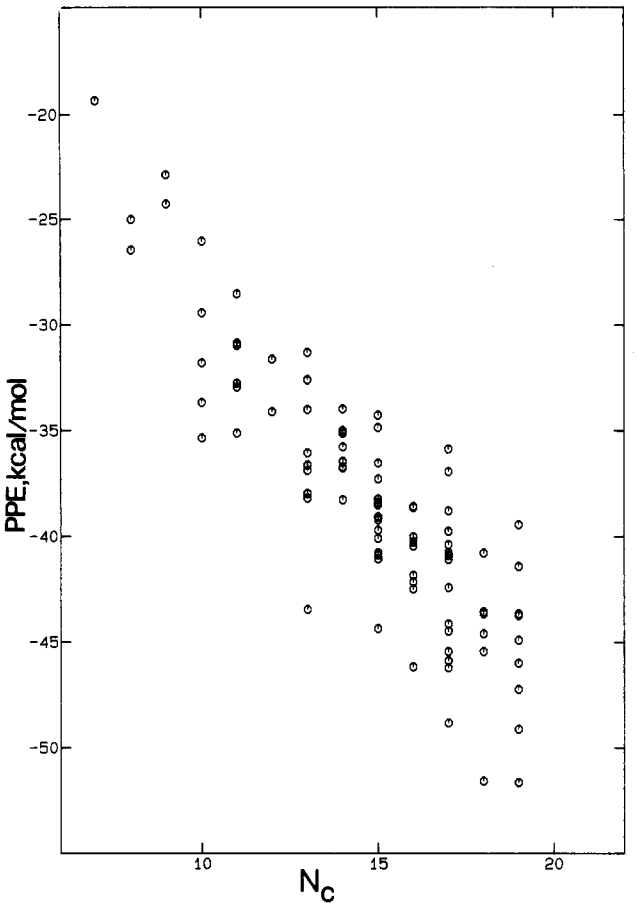

Figure 3. Plot of PPE versus the number of C atoms in the molecule for 93 compounds with C=O or C≡N groups.

TABLE IV: Average Atomic Contributions to PPE (Atomic Relevances) for Various Atoms (σ's of the Distributions in Parentheses; in kcal/mol, 7-Å Cutoff)

	$\bar{E}$		
atom	C=O crystals	C≡N crystals	hydrocarbon crystals
>C<	1.60 (29)	1.54 (31)	1.32 (37)
>C<(H)	1.94 (23)	1.83 (27)	1.76 (33)
O or N	1.73 (29)	1.62 (24)	
	13.5 (4)[a]	17.8 (1)[a]	
	6.7 (1)[b]	9.9 (1)[b]	
H	0.66 (14)	0.67 (12)	0.67 (16)
C≡(N)		1.88 (26)	
>C(H_2)	1.71 (25)	1.66 (16)	1.69 (31)
-C(H_3)	1.76 (29)	2.03 (22)	1.74 (33)

[a] Average atomic surface (Å^2). [b] Average atomic volume (Å^3).

The packing of the polar molecules considered here is, in this respect at least, but slightly perturbed by the polar substituent. Figure 4 shows a histogram of the distribution of E_i for oxygen and nitrogen; the histogram for oxygen is sharp, meaning that the contribution of the oxygen atom to the PPE is constant in different crystal structures, as required by the homomeric principle.[11] The one outlier in Figure 4a is hexa-*tert*-butylacetone, in which the oxygen atom is almost completely screened from intermolecular interactions by the bulky side groups:

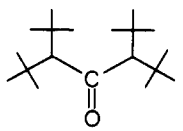

Figure 5 shows the distribution of intermolecular distances in crystals of carbonyl compounds. Short O···O contacts are absent;

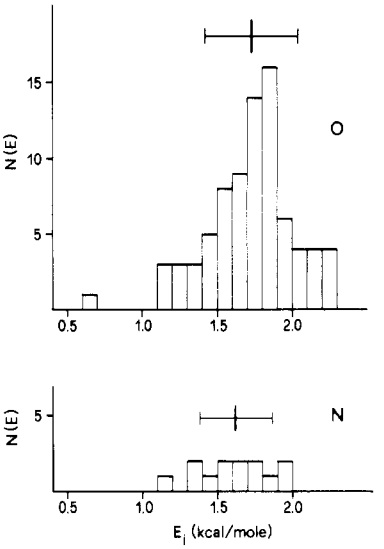

Figure 4. Histograms for the atomic contribution to PPE of an O or N atom. The vertical bar marks the average, the horizontal line the standard deviation.

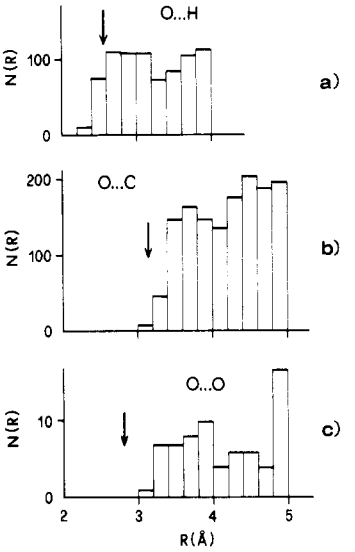

Figure 5. Histograms of the number of intermolecular distances in carbonyl crystals. The vertical arrow denotes the sum of the van der Waals radii (Table VI). Note the different ordinate scale in (c).

oxygen atoms swim in a sea of hydrophobic interactions. Also O···C contacts are distributed on the safe side of the sum of the corresponding van der Waals radii (see Appendix). Our data suggest that a proposed[12] C···O closest contact distance (3.34 Å) should be somewhat shortened. Taylor and Kennard[13] defined C—H···O hydrogen bonds by a H···O distance shorter than 2.4 Å; there are only 9 such contacts in our data set, although 84 contacts appear to be shorter than the sum of the van der Waals radii. But hydrogens have been placed in calculated positions, and therefore these short contacts may be artifacts due to this approximation. In particular, apparently short O···H distances with respect to former analyses may result from our use of a C–H distance (1.08 Å) which is longer than that usually found from X-ray crystallographic studies. Weak contributions from Coulombic forces between positive regions at H and negative regions near O are, however, possible.

Orientation of C=O and C≡N Dipoles in the Crystal. A question of both theoretical and practical relevance is whether the charge polarization in C=O or C≡N groups will induce a

(11) Gavezzotti, A. *Nouv. J. Chim.* **1982**, *6*, 443.

(12) Gould, R. O.; Gray, A. M.; Taylor, P.; Walkinshaw, M. D. *J. Am. Chem. Soc.* **1985**, *107*, 5921.

(13) Taylor, R.; Kennard, O. *J. Am. Chem. Soc.* **1982**, *104*, 5063.

TABLE V: Space Group Frequencies (%) (Total Number of Crystal Structures in Parentheses)

space group	C=O + C≡N crystals (93)	hydrocarbon crystals[a] (391)	hydrocarbon $N_C < 20$ (175)	organic crystals[b] (29059)
$P2_1/c$	39.8	42.2	42.3	36.0
$P2_12_12_1$	18.3	4.6	5.7	11.6
$P\bar{1}$	11.8	14.9	14.9	13.7
Pbca	7.5	7.7	6.9	4.3
$C2/c$	3.2	10.3	6.3	6.6
$P2_1$	2.2	4.4	5.1	6.7
others	17.2	15.7	18.9	21.1

[a] From ref 1. [b] From Mighell et al.: Mighell, A. D.; Himes, V. L.; Rodgers, J. R. *Acta Crystallogr., Sect. A* **1983**, *39*, 737.

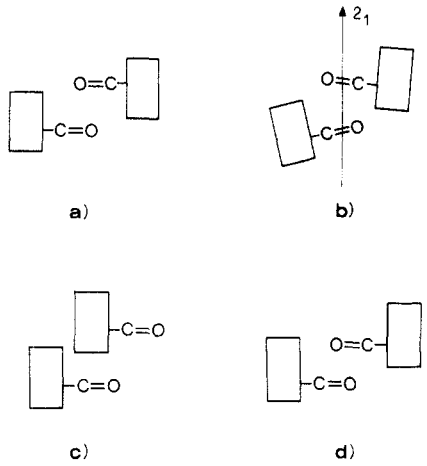

Figure 6. Generation of antiparallel dipole–dipole interactions by (a) center of symmetry and (b) screw diads. (c) Close contact between dipoles at $\theta = 0°$, with steric interactions (the hydrocarbon part of the molecule is schematized by the rectangle), and easy access for $\theta = 180°$ (d).

preferred molecular orientation in the crystal, and, in particular, whether centrosymmetric space groups are more frequent than in hydrocarbons, because of the tendency of neighboring dipoles to arrange themselves in a head-to-tail fashion according to simple electrostatic reasoning. It appears (Table V) that all the most frequent centrosymmetric space groups are less populated for the sample of polar molecules than for hydrocarbons. Particularly striking is the increase in frequency of space group $P2_12_12_1$. A simple hypothesis is illustrated in Figure 6: if dipoles are nearly perpendicular to a screw diad, a favorable antiparallel arrangement of symmetry-related dipoles can be achieved, and in that space group the three perpendicular screw axes could produce a multidimensional network of such favorable interactions, rather than just pairs, as are obtained over an inversion center.

Figure 7 shows a scatterplot of the interdipole distance (R_D) versus orientation (θ; see Figure 1). For $R_D < 5$ Å, the large majority of cases has $\theta = 180°$, with a perhaps significant subclustering around $\theta = 100°$. Antiparallel ($\theta = 180°$) dipoles may come much closer to each other than the parallel ($\theta = 0°$) ones, the distance of minimum approach, 3.15 Å, being just the sum of the C and O van der Waals radii. Except for a few outliers, the distance of minimum approach between dipole midpoints and the orientation angle are correlated by the straight line

$$R_D(\text{min}) = -0.01\ \theta + 5\ \text{Å}$$

The clustering of points at $\theta = 0°$ or 180° is the unescapable consequence of pure lattice translation or of a center of symmetry. Aside from this, no preference appears for dipole orientation in crystals, outside the forbidden zone below the straight line. The spread of θ values at $R_D > 5$ Å indicates that in many cases dipole–dipole interactions are scarcely relevant to crystal packing, since the spatial arrangement, dictated by the hydrophobic components, prevents the dipoles from interacting closely in the crystal. Thus, not unexpectedly, the orientation selection rule is effective only at short distances between dipoles. In fact, the above discussion has been conducted in terms of polar factors, but our results do not show so far compelling evidence that electrostatic forces alone are at work. The lack of points at $\theta = 0°$ may also be due to general steric factors, since if the dipoles must come very close, so must the rest of the molecule, with a consequent repulsion also between the hydrocarbon parts. Dipoles at 180°

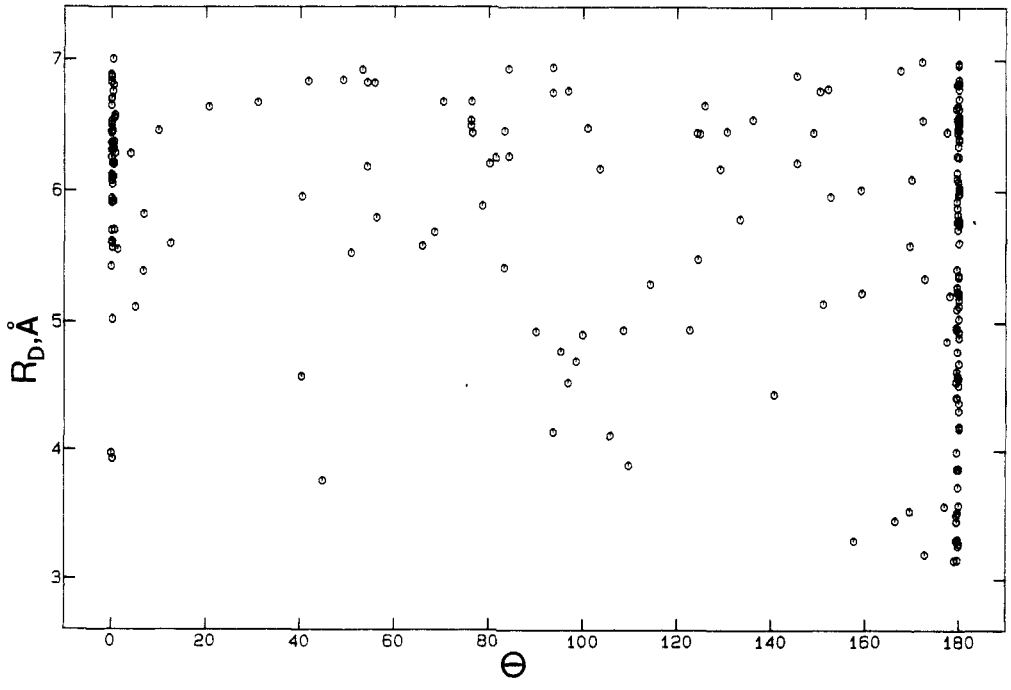

Figure 7. Scatterplot of the distance between dipole midpoints, R_D, versus θ, the angle between dipole directions (Figure 1).

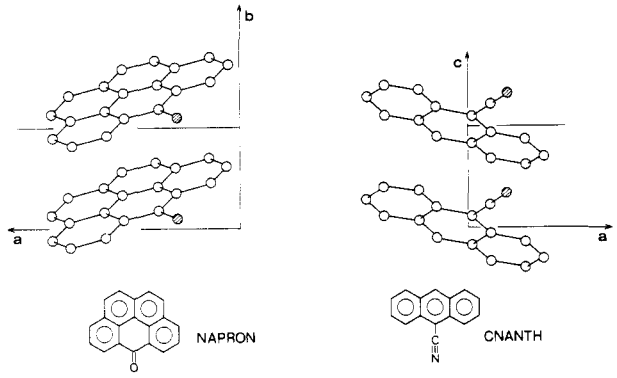

Figure 8. Parallel arrangement of C=O or C≡N dipoles (crystal structures from ref 14).

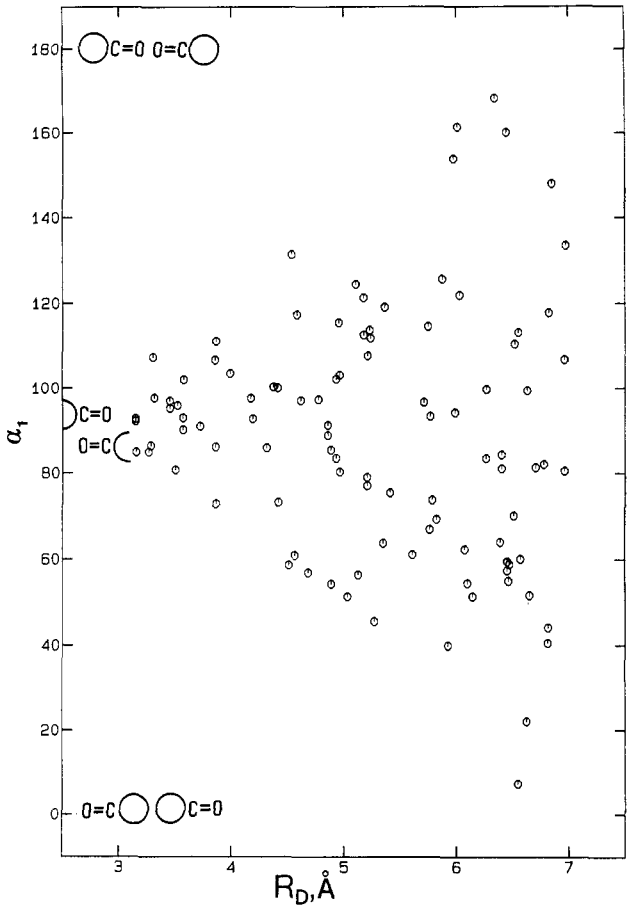

Figure 9. Scatterplot for α_1 versus R_D (Figure 1) for crystals with antiparallel dipoles (θ = 180°).

can come close to each other even if the rest of the molecule does not (see Figure 6c–d).

The outlier points at R_D = 4 Å, θ = 0° are for the molecules of naphthanthrone (NAPRON) and 9-cyanoanthracene (CNANTH), shown in Figure 8 with their packing arrangement in molecular columns.[14] In these molecules, as is usually the case for large aromatic fragments in crystals,[15] C···C attractive interactions take the lion's share, and parallel stacking at interplanar distances of 4 Å is advantageous. Thus, the electrostatic polarity constraint is overruled by other, more important, factors.

The subset of data for θ = 0° and θ = 180° allows some interesting considerations, since angles α_1 and α_2 (Figure 1) define

(14) (a) CNANTH: Rabaud, H., Clastre, J. *Acta Crystallogr.* **1959**, *12*, 1911. NAPRON: Fujisawa, S.; Oonishi, I.; Aoki, J.; Iwashima, S. *Bull. Chem. Soc. Jpn.* **1976**, *49*, 3454.

(15) (a) Gavezzotti, A.; Desiraju, G. R. *Acta Crystallogr., Sect. B* **1988**, 44, 427. (b) Desiraju, G. R.; Gavezzotti, A. *J. Chem. Soc., Chem. Commun.* **1989**, 621.

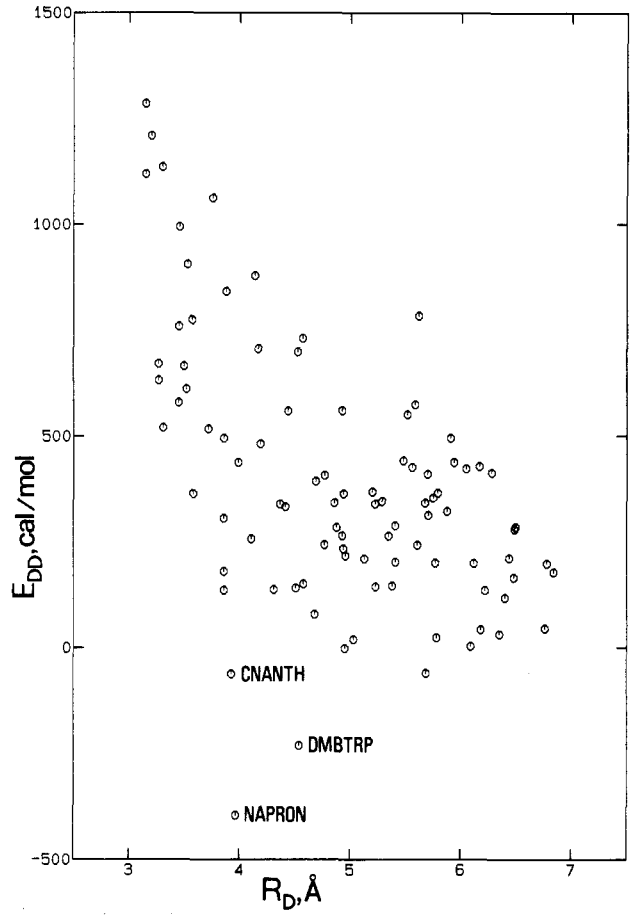

Figure 10. A plot of the dipole–dipole energy per unit charge, E_{DD}, versus the minimum dipole–dipole distance in the crystal.

the amount of offset between coplanar dipoles. At θ = 0°, there is no selectivity on α, with the only exceptions of NAPRON and CNANTH (as noted before), where, for an R_D of 4 Å, α is equal to 80° or 71°, respectively. This causes an almost exact superimposition of parallel dipoles, an electrostatically unfavorable arrangement. Figure 9 shows the population for θ = 180°; although a structure with fully head-to-head dipoles (α_1 = 180°, R_D = 4 Å) would still be compatible with the sum of the van der Waals radii, α_1 values converge to 90° at short R_D, corresponding to the electrostatically favorable superimposition of head-to-tail dipoles. Therefore, carbonyl or nitrile dipoles never point directly to each other in crystals; and this must be a purely electrostatic effect, since the steric hindrance of the molecule would not prevent such an arrangement. Ordinary steric factors are on the other hand at work in the lower part of the graph in Figure 9, since at α_1 = 0° the rest of the molecule is interposed between the dipoles, and small R_D values are impossible for this reason.

Dipole–Dipole Electrostatic Energies. The dipole–dipole lattice potential energy, E_{DD}, was computed as

$$E_{DD} = \sum_j \frac{1}{\epsilon} \frac{1}{4\pi\epsilon_0} q^2 \left\{ \frac{\bar{v}_0 \cdot \bar{v}_j}{|R_D|^3} - \frac{3(\bar{v}_0 \cdot \bar{R}_D)(\bar{v}_j \cdot \bar{R}_D)}{|R_D|^5} \right\}$$

where ϵ is the unknown dielectric constant of the medium (taken equal to 1), q is the dipole charge, and $\bar{v}_0$ and $\bar{v}_j$ are the reference and symmetry-related dipole vector, respectively (see Figure 1). The summation was extended to include all dipoles with ±2 unit cells from the reference molecule (125 unit cells). Convergence of the summation was not thoroughly checked, since only relative values of E_{DD} are of interest here, but test calculations showed that enlarging these limits causes only minor variations in E_{DD}. A unit charge q was assumed; it is of course very easy to rescale E_{DD} to any charge separation. E_{DD} is usually a negative (stabilizing) quantity, but may be repulsive in some cases, when no favorable dipole–dipole orientation is reached in the crystal. For

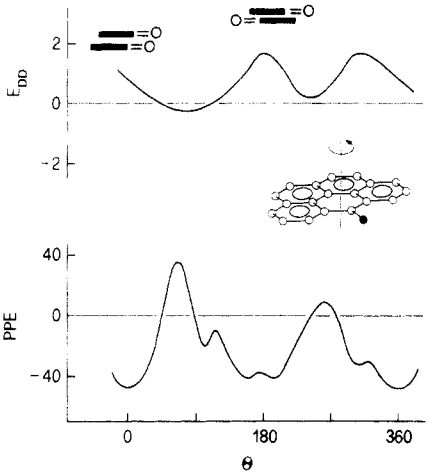

Figure 11. PPE and E_{DD} profiles (kcal/mol) for the rotation of one molecule of naphthanthrone around its axis of maximum inertia, in a fixed crystal environment. Dipole–dipole energy calculated for a dipole charge of 0.3 electron.

an order-of-magnitude estimate, we report that the average E_{DD} is −8.6 (70) kcal/(mol·electron), while the average 6-exp energy is −38.3 (62) kcal/mol. Since reasonable charge values in organic bonds are a few tenths of an electron, E_{DD} in our crystals can be estimated at about, or less than, 2 kcal/mol on the average.

E_{DD} can be used as an indicator of the favorable arrangement of dipoles in crystals. Figure 10 shows a scatterplot for this quantity against the closest-neighbor dipole–dipole distance. The plot shows that having at least one short dipole-dipole contact is a necessary but not sufficient condition for a relatively large E_{DD}, as demonstrated by the lack of data points in the upper right part of the graph. A large fraction of the crystal structures in our sample has R_D(min) larger than 5 Å, and an almost negligible E_{DD}, and can therefore be said to be relatively insensitive to the presence of the dipoles. The distribution of E_{DD} is also insensitive to molecular size.

The unfavorable electrostatic terms in the structures of NAPRON and CNANTH are clearly borne out in Figure 10. The repulsive dipole–dipole energy for CNANTH is small, indicating attractive interactions with dipoles further apart than the closest ones, while for NAPRON the nearest-neighbor repulsive interaction is dominant. The stabilization provided by aromatic core overlap is responsible for the parallel arrangement of the molecules, but it remains to be explained why this is not achieved with antiparallel dipoles. Figure 11 shows that the observed packing exerts a considerable electrostatic force on the molecule, since the E_{DD} profile has a substantial first derivative; at the same time, a 180°-rotated guest is a rather inexpensive defect even in the observed packing. Remarkably, however, such a guest finds itself in an unfavorable electrostatic environment too (E_{DD} is repulsive). While we cannot propose a unique explanation for the observed packing, this example illustrates the subtle balance of factors upon which packing depends. In this respect, the case of the other crystal for which E_{DD} is repulsive, 2,7-dimethyl-4,5-benzotropone (DMBTRP20), is instructive:

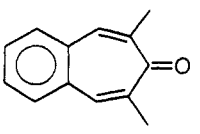

These molecules pack in a parallel fashion,[16] as predicted[1] for rigid cylindric molecules, with repulsive interactions between adjacent dipoles, even if there is no overlap at all between the aromatic cores.

A plot of E_{DD} versus the θ angle for nearest-neighbor dipole–dipole contacts shows no forbidden areas, but a clustering (54%) at $\theta > 170°$, mostly (but not exclusively) corresponding to inversion-center-related couples. On the other hand, 62% of the structures have at least one dipole–dipole contact shorter than 7 Å with $\theta > 170°$. These percentages show that head-to-tail arrangements of C=O and C≡N dipoles in crystals are frequent, but by no means compulsory.

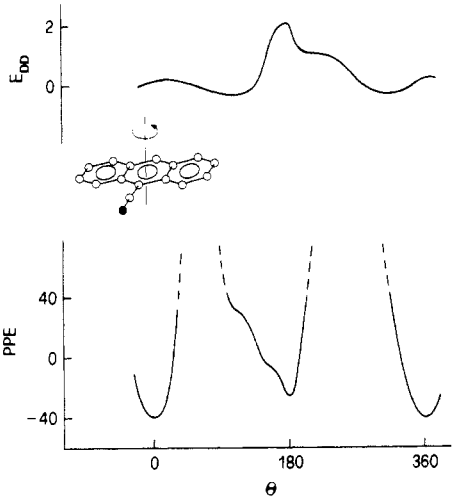

Figure 12. Same as Figure 11, for 9-cyanoanthracene.

Mention of Previous Work. A survey of packing modes for carbonyl (quinonoid) compounds has been carried out by Bernstein, Cohen, and Leiserowitz.[17] These authors identify a tendency of quinone molecules to stack, giving short repeat distances of about 4 Å. Besides, they identify at least two common types of interactions between carbonyl groups in crystals, as in the scheme below:

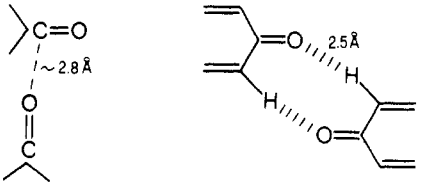

The first type seems not to be present in our sample, which has no O···C distances below 3 Å (Figure 5). As for the second, hydrogen-bonded type, it is pointed out that it may rely upon the acidic nature of quinone ring hydrogens and therefore need not apply to our molecules (see also the previous discussion on C—H···O bonding). More relevant to our case is the finding that a number of crystals with parallel dipoles at short distances appear, due to the previously mentioned stacking propensity of quinone molecules. This is ascribed to favorable forces from overlap of aromatic cores, and our analysis in the foregoing sections agrees with this interpretation.

A survey of O···C=O interactions in organic crystals, aimed at revealing incipient reaction centers, was carried out by Buergi, Dunitz, and Shefter,[18] who concluded that no such effect is present for O···C distances longer than 3 Å; therefore, there are none in our sample (see Figure 5b).

The 9-cyanoanthracene crystal has been studied extensively due to its peculiar properties and solid-state dimerization that leads to the trans product in spite of the cis location of reacting centers.[19] Orientational disorder, further testifying to the competition between packing forces, was detected. Figure 12 shows that the situation is analogous to that found for naphthanthrone (Figure 11), although the rotational barrier is too high for the process to be a dynamic one in the crystal.

(16) Ibata, K.; Shimanouchi, H.; Sasada, Y. *Acta Crystallogr., Sect. B* **1976**, *32*, 2054.

(17) Bernstein, J.; Cohen, M. D.; Leiserowitz, L. In *The Chemistry of the Quinonoid Compounds*; Patai, S., Ed.; Wiley: London, 1974; pp 83–105.

(18) Buergi, H.-B.; Dunitz, J. D.; Shefter, E. *Acta Crystallogr., Sect. B* **1974**, *30*, 1517.

(19) See for a discussion: Wright, J. D. *Molecular Crystals*; Cambridge University Press: Cambridge, U.K., 1987; pp 44–49.

TABLE VI: Empirical Parameters for Nonbonded Interactions (kcal/mol)[a]

contact	A	B	C	van der Waals radius, Å
C···C	71 600	3.68	421	1.75
O···O	77 700	4.18	259.4	1.40
N···N	42 000	3.78	259	1.55
H···H	4900	4.29	29	1.17
C···O	75 700	3.91	339.4	
C···N	55 300	3.73	331.4	
C···H	18 600	3.94	118	
O···H	19 500	4.23	88	
N···H	14 400	4.00	91	

[a] From ref 5; as discussed also in refs 1 and 6.

Conclusions

A survey of the packing energies and packing modes of crystals containing one C=O or C≡N group per molecule, in comparison with hydrocarbon crystals, reveals the following:

1. The calculated packing energies, both integral and partitioned into contributions from each atom, reveal amost no perturbation by the polar substituent. No clear proof of C—H···O interactions appears.

2. The oxygen atom conforms to the homomeric principle, giving a contribution of 1.73 (29) kcal/mol to the PPE in any crystal; the restricted database does not allow a similar check for nitrogen.

3. Aside from $P2_1/c$, the (noncentrosymmetric) space group $P2_12_12_1$ is the most frequent in these crystals; the presence of the dipole does not therefore increase the chances of having a centrosymmetric space group.

4. Near-neighbor parallel dipoles are generally forbidden, but exceptions appear when stronger driving forces are present. Steric hindrance from the rest of the molecule may also prevent this arrangement.

5. C=O or C≡N dipoles never point oxygen to oxygen or nitrogen to nitrogen in crystals, due to the unfavorable electrostatic interaction.

6. If the dipole–dipole energy is taken as a rough approximation to the electrostatic potential in the crystal, it is seen that having short dipole–dipole distances is a necessary, but not sufficient, condition for a large electrostatic cohesion energy, since near-neighbor dipoles may have unfavorable mutual orientations. Also, many crystals have large dipole–dipole distances and quite negligible electrostatic energies.

Acknowledgment. Partial financial support from Ministero della Pubblica Istruzione, Fondi 40%, is acknowledged. We thank the Servizio Italiano di Diffusione Dati Cristallografici del CNR (Parma) and Dr. T. Pilati for the handling of the Cambridge Structural Database, and Prof. E. Ortoleva for use of his plotting programs. Calculations have been performed on a Gould NP1 minisupercomputer.

Appendix

Packing potential energies were calculated by using atom–atom nonbonded potential energy formulas, as

$$\mathrm{PPE} = 2\mathrm{PE} = \sum_i \sum_j A \exp(-BR_{ij}) - CR_{ij}^{-6}$$

Note that PPE as defined above was instead called PE in ref 1. A, B, C are empirical parameters (Table VI), R_{ij} is an intermolecular distance between atom i of a reference molecule and atom j in the surrounding, symmetry-related molecules, within a 7-Å cutoff limit. Bulk moduli, K_0 (at zero-pressure limit and at 60% of the melting temperature), and reduced thermal conductivities, λ_T, were calculated by using approximate formulas[20] which have been previously discussed.[1]

The molecular surface and volume were calculated assuming interlocking spheres with radii as in Table VI. The effective surface,[2] S_{eff}, was calculated by artificially setting the van der Waals radius for C or O atoms at 2.50 Å, and neglecting the hydrogen atoms. This inflated surface approximates more closely the accessible molecular surface.

Supplementary Material Available: Table I, listing Cambridge Structural Database refcodes for C=O- and C≡N-containing crystals (1 page). Ordering information is given on any current masthead page.

(20) Bondi, A. *Physical Properties of Molecular Crystals, Liquids and Glasses*; Wiley: New York, 1968; Chapters 4 and 5.

^{57}Fe Mössbauer Spectroscopy of the FeS Cathode in the Li/FeS Battery System

C. H. W. Jones,* P. E. Kovacs, R. D. Sharma, and R. S. McMillan†

Department of Chemistry, Simon Fraser University, Burnaby, British Columbia, Canada V5A 1S6
(Received: July 26, 1989; In Final Form: October 27, 1989)

The mechanism of discharge of the Li|$LiAsF_6$–propylene carbonate|FeS battery system has been studied by ^{57}Fe Mössbauer spectroscopy of the cathode. The only product identifiable in the cathode reduction appears to be iron, some of which is present as small particles that exhibit superparamagnetism. There is no evidence for macroscopic amounts of a lithiated intermediate.

Introduction

The use of iron sulfides as cathodes in high-energy-density batteries has been of interest for some time.[1,2] We have previously studied FeS_2 as a cathode material by Mössbauer spectroscopy[3] and in this paper report on FeS and its behavior on discharge in the Li|$LiAsF_6$–propylene carbonate|FeS systems, again employing ^{57}Fe Mössbauer spectroscopy as the analytical tool.

In the high-temperature (450 °C) Li/FeS battery system, where the electrolyte was a molten LiCl/KCl eutectic, Tomczuk et al.[4] proposed, on the basis of X-ray diffraction measurements, etc., that two mechanisms were operative, one leading to Li_2FeS_2 as an intermediate and the other $LiK_6Fe_{24}S_{26}Cl$ (J phase). The former mechanism was favoured by higher temperature and LiCl concentrations. Metallographic examination of FeS cathodes

† National Research Council, Ottawa, Ontario, Canada.

(1) Clark, M. B. In *Lithium Batteries*; Gabano, J. P., Ed.; Academic: New York, 1984; p 115.
(2) Vissers, D. R. In *Materials for Advanced Batteries*; Murphy, D. W., Broadhead, J., Steele, B. C. H., Eds.; Plenum: New York, 1980; Vol. 2, p 47.
(3) Jones, C. H. W.; Kovacs, P. E.; Sharma, R. D.; McMillan, R. D., in press.
(4) Tomczuk, Z.; Preto, S. K.; Roche, M. F. *J. Electrochem. Soc.* **1981**, *128*, 760.

0022-3654/90/2094-4325$02.50/0